Spin filtering and an enhanced regime of giant magnetoresistance

2000 J. Phys.: Condens. Matter 12 2833

(http://iopscience.iop.org/0953-8984/12/12/322)

J. Phys.: Condens. Matter **12** (2000) 2833–2846. Printed in the UK PII: S0953-8984(00)08749-X

Spin filtering and an enhanced regime of giant magnetoresistance

M S Ferreira†, J d'Albuquerque e Castro†, R B Muniz† and Murielle Villeret‡

† Departamento de Física, Universidade Federal Fluminense, Niterói, Brazil
‡ Department of Mathematics, City University, London EC1V 0HB, UK

Received 15 October 1999, in final form 7 January 2000

Abstract. A new regime of magnetoresistance (MR) in systems composed of magnetic layers separated by non-magnetic modulated structures is studied. The ability to tailor the electronic structure of superlatticed systems enables one to engineer contrasting spin-dependent transport properties, enhancing the magnetoresistance ratios. When the system acts as a spin filter the MR ratios reach values many orders of magnitude larger than those of conventional giant magnetoresistance. Rather than a mere enhancement of the magnetoresistance ratios, this new regime involves ingenious combinations of spin-polarized currents. Moreover, it results from a magnetic-field-induced metal–insulator transition along the modulation direction, characterizing a highly anisotropic transport behaviour. The existence of an insulating phase circumvents the experimental challenge of probing excessively small resistances in the current-perpendicular-to-plane (CPP) geometry of magnetoresistance. A picture in terms of the bulk Fermi surfaces of the constituent materials emerges and provides general guidelines on how to achieve this regime.

1. Introduction

Basic research in the physical sciences, particularly in condensed matter physics, has led to important developments in applied physics, engineering and ultimately in industry. One good example is the production and commercialization [1] of magnetic sensors and read heads based on the giant magnetoresistance (GMR) effect. The GMR effect, discovered only a decade ago [2], is characterized by a striking change in electrical resistance of metallic systems due to an external magnetic field. It was originally found in multilayered structures, although it has also been observed in other systems, such as granular materials [3]. In multilayers, the magnetizations of magnetic layers separated by non-magnetic materials can be either parallel (P) or antiparallel (AP), depending on the thickness of the latter [4]. The electrical resistance of the system depends on the orientation of the magnetizations and therefore, by applying a magnetic field to a multilayer whose magnetizations are antiparallel, one can align them and affect its electrical resistance. Likewise, in granular materials, magnetic grains embedded in non-magnetic metallic hosts may have their moments aligned by an applied magnetic field with a consequent change in the resistance of the system. In either case, it is clear that the more sensitive the resistance as a function of the relative orientation of the moments, the larger the MR. There is a consensus that the origin of the effect is in the spin-dependent scattering of the electronic carriers [5], which is the key to understanding GMR and other related phenomena. In fact, spin-polarized transport has become the focus of several studies over the past few years [6].

0953-8984/00/122833+14$30.00

Bearing in mind the continuing effort to manufacture high-quality magnetic sensors and read heads, one seeks systems with large values of magnetoresistance (MR) combined with small saturating magnetic fields [7]. These fields are usually determined by the strength of the coupling between the magnetizations, which has been intensively studied in multilayered structures [4]. At low temperatures, high values of MR ranging from 100% to 220% have been reported [8], but with sizable magnetic fields. This range of MR ratios has been obtained with conventional multilayered structures, where the non-magnetic layer separating the magnetic material consists of a single metal. Theoretical predictions indicate that the MR can be enhanced by considering a number of repeats of magnetic and non-magnetic metallic layers with small thickness fluctuations [9], but the saturating magnetic fields remain of the same order of magnitude. Alternatively, percentages of hundreds of thousands are also possible within the so-called colossal magnetoresistance (CMR) regime that arises in manganese perovskites. However, the magnetic field necessary to produce the CMR can be as large as 5 T [10, 11].

Here we present a detailed study of a new transport regime, hereafter referred to as enhanced giant magnetoresistance (EGMR), characterized by large values of MR ratios obtained with small saturating fields, a highly attractive combination from the technological viewpoint. Such large MR ratios may arise in magnetic materials separated by non-magnetic modulated structures and result from a spin-filtering effect leading to highly contrasting spin-dependent transport properties. The modulation of the non-magnetic spacer introduces additional quantum interference effects within the structure and is chiefly responsible for the occurrence of the EGMR. The enhancement of the magnetoresistance ratio involves ingenious combinations of the spin-polarized currents and should be distinguished from existing regimes. In fact, it results from a metal–insulator transition only along the modulation direction, characterizing a highly anisotropic electric behaviour.

The sequence adopted in this paper is as follows. In the next section we discuss the magnetoresistance effect in the ballistic regime; this is followed by a description of the model. We present a picture based on the bulk Fermi surfaces of the constituent materials which provide general guidelines on how to suppress the conductance along a certain propagation direction. Such anisotropy in the transport properties, when combined with spin-polarized currents, results in spin-filtering effects that can enhance the MR ratio leading to a new regime, which is discussed in section 3.

2. Magnetoresistance and ballistic transport

For a multilayer made of two layers of a magnetic material separated by a non-magnetic metallic spacer, the resistance of the system depends on whether the magnetizations are P or AP. The magnetoresistance is defined as the relative difference between the resistances in the two configurations, i.e., $\mathrm{MR} = (R_{AP} - R_P)/R_P$. In terms of the conductances Γ, the MR can be written as $\mathrm{MR} = (\Gamma_P - \Gamma_{AP})/\Gamma_{AP}$. The MR can be probed in the current-in-plane (CIP) and the current-perpendicular-to-plane (CPP) geometries. In the former the current flows in the direction parallel to the layers and the MR is, in general, smaller than that of its perpendicular counterpart. Although in principle larger, the MR in the CPP geometry is experimentally more challenging because the layers usually consist of very thin films, which makes the resistances along the perpendicular direction very small and difficult to measure [5]. In this paper we will be concerned with the CPP magnetoresistance in multilayers where the non-magnetic spacer has a modulated structure. In this case we show that the problem of extremely small resistances is circumvented by the appearance of an insulating phase that arises in the EGMR regime, making the resistances involved not as small as those of conventional CPP structures.

As far as the spin-polarized currents are concerned, it is convenient to consider the

spin-quantization axis along the magnetization direction of one of the magnetic layers. Without spin-flip scattering the resistances for each spin channel are added in parallel, i.e., the total conductance is a simple sum of the spin-polarized conductances ($\Gamma = \Gamma^{\uparrow} + \Gamma^{\downarrow}$). It is evident from the definitions above that the more contrasting the conductances between the P and AP configurations, the larger the MR ratio. The contrast in the total conductance Γ reflects, in turn, the contrast between the spin-polarized conductances $\Gamma_P^{\uparrow}$ and $\Gamma_P^{\downarrow}$. In the AP configuration the spin-polarized conductances are the same and there is no contrast between them. However, the larger the difference between $\Gamma_P^{\uparrow}$ and $\Gamma_P^{\downarrow}$, the smaller the Γ_{AP}, leading to larger MR ratios. Notice therefore that the ideal situation for MR is that of a perfect spin filter in which carriers are transmitted for a certain spin polarization but blocked otherwise. In fact, there are continuing efforts to find 100%-spin-polarized conducting materials, which, depending on the direction of the magnetization relative to the spin polarization of the current, can function either as conductors or as insulators [1].

The ability to produce increasingly smaller electronic devices enables one to obtain conductances within the so-called ballistic regime. In contrast to diffusive transport, where phonons and defects play important roles in the scattering of carriers, the ballistic regime is characterized by sample dimensions smaller than the mean free path of the carriers. In this case transport properties are primarily determined by the electronic structure and the geometry of the system in the absence of impurities and/or disorder. Within the Landauer–Büttiker formalism the CPP conductance per unit area for crystalline layers with sharp interfaces at zero temperature is given by [5, 12]

$$\Gamma = \frac{e^2}{h} \int \frac{\mathrm{d}\vec{k}_{\parallel}}{4\pi^2}\, T(\vec{k}_{\parallel}, E_F) \tag{1}$$

where $\vec{k}_{\parallel}$ is the wave vector parallel to the layers, E_F is the Fermi energy, $T(\vec{k}_{\parallel}, E_F)$ is the transmission coefficient of carriers across the system, e is the electron charge and h is the Planck constant. The integration over $\vec{k}_{\parallel}$ reflects the absence of diffusive scattering which makes $\vec{k}_{\parallel}$ a conserved quantity. An alternative way of looking at $\vec{k}_{\parallel}$ is that, as a good quantum number, it represents independent transport channels or modes. Each of these channels may or may not contribute significantly to the total conduction across the system, depending on whether the corresponding states along the modulation direction are extended or evanescent, respectively. In the latter, exponentially decaying states along the modulation direction contribute to the conduction only by tunnelling. Such a contribution is negligible compared to those of the extended states.

Up to this point, no particular information about the spacer was needed. Here we assume that the non-magnetic spacer is composed of a superlatticed structure made of two layers A and B, having respective thicknesses a and b, periodically juxtaposed. The system that we consider is represented schematically in figure 1. To illustrate the conditions for the occurrence of the EGMR regime we describe the electronic structure within the free-electron model, so that electrons are free to move along the in-plane directions and feel a Kronig–Penney-like potential along the modulation direction. The carrier motion is then split into components parallel and perpendicular to the layers, with energies $E_{\parallel} = \hbar^2 k_{\parallel}^2/2m$ and $E_{\perp}$, respectively. This may be a simplified description of the electronic structure, particularly for systems based on transition metals, where sp–d hybridization effects can be very important. However, from a qualitative point of view, it contains the basic ingredients necessary for understanding how the EGMR regime can be established, and is sufficient to explain the main issues involved.

Figure 2 displays a typical set of spin-polarized potential profiles felt by electrons along the modulation direction. The potential depends both on the spin polarization and on the magnetic configuration of the system. The set of four profiles corresponds to both spin-polarized

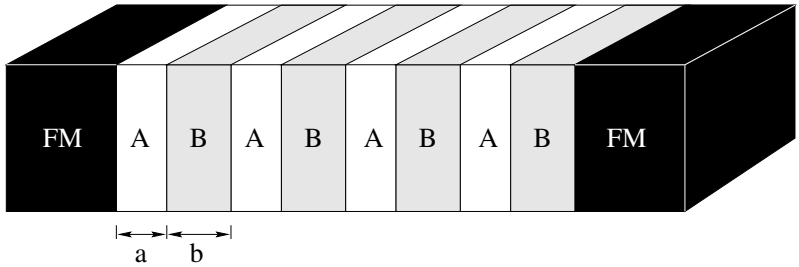

Figure 1. A schematic representation of the multilayered system. Two magnetic layers sandwich a superlatticed spacer composed of layers A and B periodically juxtaposed.

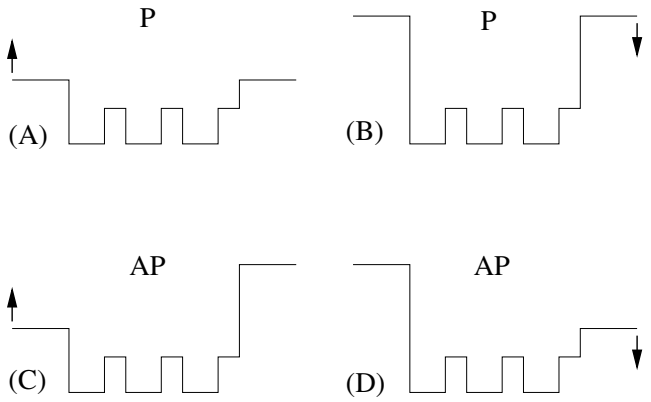

Figure 2. A schematic representation of the potential profiles along the modulation direction felt by ↑- and ↓-spin electrons in the P and AP configurations.

electrons in both magnetic configurations. The upper and lower profiles correspond to the P and AP configurations, respectively; the left-hand curves represent the profiles felt by ↑-spin electrons and the right-hand ones those felt by ↓-spin electrons. The potential within the modulated spacer is independent of the spin polarization but assumes different values within the magnetic material, being either $V_\uparrow$ or $V_\downarrow$. For the sake of illustration, in figure 2, $N_c = 3$ is the number of cells (or bilayers) in the modulated spacer whose potentials are V_A and V_B in the A and B regions, respectively.

According to equation (1), the CPP conductance reduces to a sum over $\vec{k}_\parallel$ of solutions of independent one-dimensional problems involving the evaluation of transmission coefficients $T(\vec{k}_\parallel, E_F)$, which can be obtained using elementary quantum mechanics methods. In fact, transfer-matrix techniques are widely used to obtain transmission coefficients across quantum heterostructures [13–15]. In the appendix, we show one of these techniques and obtain expressions for the transmission coefficients. For the electron-gas model we have that $T(\vec{k}_\parallel, E_F) = T(E_F - E_\parallel) = T(E_\perp)$. Figure 3 shows a typical curve of the transmission coefficients as a function of the perpendicular energy component $E_\perp$. It illustrates the majority-spin electron transmission coefficient in the P configuration ($T_P^\uparrow$), corresponding to the potential profile of figure 2(a). The parameters used are $V_\uparrow = 0.12$, $V_A = 0$, $V_B = 0.12$, $a = b = 4$ and $N_c = 30$. Here, energies and lengths are measured in atomic units. Figure 3 shows a distinct transmission gap corresponding to certain energies with which carriers cannot propagate across the structure. Those forbidden energies result from the Kronig–Penney mini-band structure

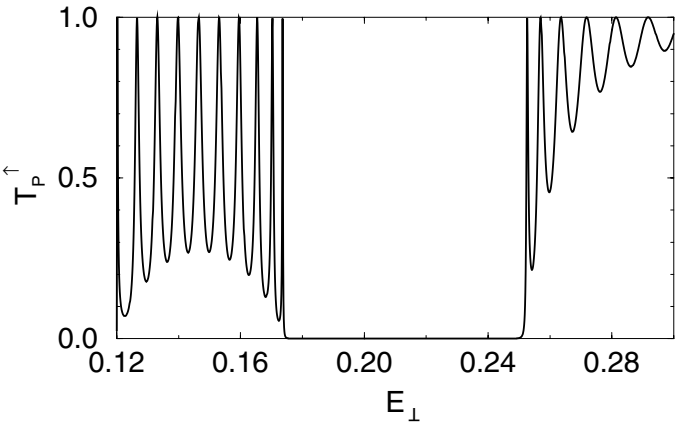

Figure 3. The transmission coefficient of ↑-spin electrons in the P configuration as a function of $E_{\perp}$.

originated within the modulated spacer, which suppresses the carrier propagation along the perpendicular direction. The existence of these forbidden transmission channels is not an exclusive feature of the simple one-band model used to describe the electronic structure of the modulated spacer. In fact, their presence is relatively common, and can be found in realistic band structures of several superlattices [5]. For modulated structures based on transition metals, the locations and sizes of the non-conducting channels, as well as the CPP MR, may be strongly affected by sp–d hybridization. Quantum reflections at the interfaces of the modulated structure generating such gaps, for example, can be substantially enhanced by sp–d hybridization effects. Therefore, a quantitative analysis of the ballistic transport across those systems would certainly require adequate treatment of such effects. However, it is worth stressing that from a qualitative point of view, one may ignore some of the details that cause the transmission gaps, and approximately simulate their appearance using a simple one-band model and a suitable Kronig–Penney-like potential profile to describe the modulated structure. In this case, the sizes and positions of the non-conducting channels are solely regulated by the heights and widths of the Kronig–Penney potential. More specifically, their positions are determined by the modulation periods and their sizes by the strength of the potentials involved [5]. The key point here is the existence of gaps in the total CPP transmission across modulated structures, and that we can use them to prevent carriers with a certain spin polarization from being transmitted across the structure. As previously stated, this will enhance the contrast between the spin-polarized currents and increase the MR ratio.

The conductance depends on the transmission coefficients only at the Fermi level and, for a given E_F, the parallel and perpendicular energies are related by $E_{\perp} = E_F - E_{\parallel}$. The integral over $\vec{k}_{\parallel}$ can thus be replaced by summing the transmission coefficient over $E_{\perp}$ up to E_F. Therefore, a simple qualitative analysis of the conductance is possible by looking at the transmission coefficient curve. There will be a finite conductance whenever at least one transmission band lies below the Fermi level. In figure 3 for instance, $E_{\perp}$ is varied from $V_{\uparrow} = 0.12$, the highest potential in this case, onwards. Notice that wherever E_F is, there will always be a lower transmission band which makes the system conduct. If no transmission bands lay below E_F, the conductance would vanish and the system would act as an insulator. This can occur if the lowest transmission band in figure 3 is suppressed and the Fermi level lies within the transmission gap [12]. We emphasize that such an insulating behaviour would

occur only along the modulation direction since carriers are free to move along the in-plane direction. This highly anisotropic property of the system, as we shall see, is essential for the appearance of the EGMR effect.

To understand how the lowest transmission band can be suppressed, we now describe a picture that establishes the correspondence between the transmission coefficients and the Fermi surfaces of both magnetic and non-magnetic bulk materials. This picture provides general guidelines for the adequate selection of spin-polarized electronic structures that give rise to the EGMR regime. Gaps in the transmission coefficients indicate the absence of extended states along the modulation direction. We recall that $E_\perp = E_F - E_\parallel$. Thus, for a given E_F, a transmission gap in the $E_\perp$-axis corresponds to a range of $\vec{k}_\parallel$-channels for which there is no conductance. Bearing in mind that transmission through the entire structure implies propagating modes across each of its individual components, we need to identify those channels with extended states both in the magnetic material and in the modulated spacer. Those states can be identified from the separate bulk Fermi surfaces. As far as the magnetic material is concerned, we have two spin-polarized Fermi surfaces, one for $\uparrow$-spin and one for $\downarrow$-spin which, within the electron-gas model, are simple closed spheres of different diameters. When projected on the in-plane direction both surfaces become concentric disks indicating those $\vec{k}_\parallel$-channels that conduct across the magnetic material. The spacer Fermi surface, on the other hand, may develop openings along the modulation direction, reflecting the absence of extended states for certain $\vec{k}_\parallel$-channels. When projected, these openings become disks and/or rings of non-conducting channels. The existence of the openings is relatively common, and can be found in a number of modulated structures [5]. For such values of $\vec{k}_\parallel$, the associated wave vectors of the spacer Fermi surface along the modulation direction are not real and correspond to evanescent states. Whether the openings are centred disks or rings of non-conducting channels in the projected Fermi surface depends on the position of the transmission gaps relative to the Fermi level.

To illustrate the relationship between the transmission coefficients and the bulk Fermi surfaces of the constituent materials, consider the transmission $T_P^\uparrow$ of figure 3. If the Fermi level lies within the transmission gap, for instance $E_F = 0.23$, there will be no extended states along the modulation direction for small values of $\vec{k}_\parallel$ (i.e. $E_\perp \approx E_F$). That corresponds to a region of non-conducting channels in the projection of the spacer Fermi surface on the in-plane direction, which is represented in figure 4(b) by a centred white disk. As $E_\perp$ is lowered, $E_\parallel$ is increased ($E_\parallel + E_\perp = E_F$), and so are the values of $k_\parallel$. When $E_\perp$ leaves the gap, extended states along the modulation direction appear and the corresponding $\vec{k}_\parallel$-channels become conducting. Those regions of conducting and non-conducting channels are schematically represented in the projected spacer Fermi surface in figure 4(b) by the hatched and white regions, respectively. Figure 4(a) shows the projected majority-spin Fermi surface of the magnetic material. The hatched disk indicates the range of conducting $\vec{k}_\parallel$-channels across the magnetic layer for majority-spin electrons. The total conductance depends on the conducting channels that are common to the magnetic layer and the modulated spacer. If a channel is conducting across the magnetic material but not across the spacer, it is counted as a non-conducting mode through the system. Similarly, it is not enough to be transmitted across the spacer if there are no conducting counterparts in the magnetic structure. It is essential to have propagating states across both materials. By projecting the Fermi surfaces of the modulated spacer and of the magnetic material on the $\vec{k}_\parallel$-plane one can see whether there are common channels across the entire structure giving rise to conductance. Figure 4(c) is a superposition of the vertically hatched channels of figure 4(a) and the horizontally hatched ones of 4(b). Since the majority-spin Fermi surface of the magnetic material is larger than the

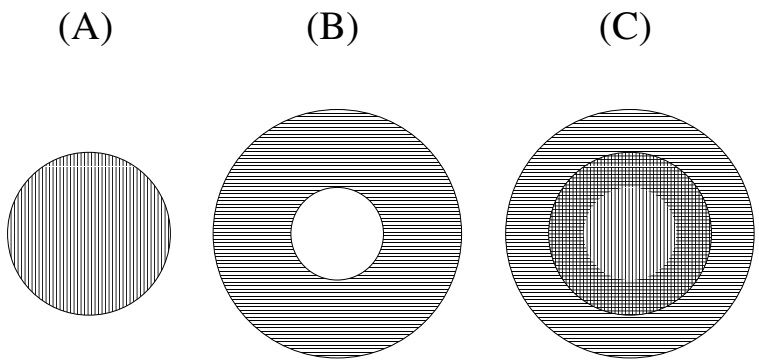

Figure 4. Schematic representations of the Fermi surfaces projected in the parallel direction. Hatched and white regions represent propagating and non-propagating channels, respectively. (a) The majority-spin Fermi surface of the magnetic material; (b) the Fermi surface of the modulated spacer; (c) the superposition of (a) and (b).

centred opening of the spacer Fermi surface, we end up in figure 4(c) with a cross-hatched ring of common conducting channels across the entire system and those are the only channels that contribute to the conductance.

From the above picture, the necessary conditions for making the conductance vanish across the system, or in other words, for suppressing the lowest transmission band, become clear. The magnetic Fermi surface has to fit into the centred opening of the spacer Fermi surface to suppress all common conducting channels. One possibility is to enlarge the centred disk of non-conducting channels in the spacer Fermi surface. This corresponds to enlarging the gap between the Kronig–Penney mini-bands that contains the Fermi level, which can be done by tuning the potential heights and/or the modulation periods. Alternatively, one could shrink the magnetic Fermi surface by reducing the carrier concentration. Either way, the lack of common conducting channels suppresses the associated conductance. It is worth stressing that in this situation, despite the non-conducting character of the system, the separate components are metallic, having their own bulk Fermi surfaces. Moreover, electrons are free to move in the parallel direction, but are allowed to travel along the modulation direction only across a few conducting channels, which characterizes a highly anisotropic behaviour. The picture based on the Fermi surfaces is useful in providing guidelines on how to suppress the lowest transmission band and the conductance along the modulation direction.

3. Spin filtering and EGMR

As mentioned before, the ideal situation corresponding to infinitely large MR ratio would be a perfect spin filter in which carriers are transmitted for a certain spin polarization but blocked otherwise. With the picture suggested above we can easily produce this filtering effect. The Fermi surface of the magnetic material is split into majority- and minority-spin parts. They are spheres with different diameters, the smallest corresponding to the minority-spin Fermi surface. The spin-polarized electronic structures can be adjusted so that the projected Fermi surfaces of the minority spin of the magnetic material and of the modulated spacer have no common transmission channels. In other words, the smallest sphere fits into the opening of the spacer Fermi surface. In this case there is no conduction and the system acts as an insulator for carriers with this spin polarization. As far as the other spin polarization is concerned,

the somewhat larger Fermi surface of the magnetic material overlaps with that of the spacer and common transmission channels give rise to a sizable conductance across the system. Therefore, we have a spin filter that conducts one type of spin-polarized electrons but not the other. To illustrate this point we have used equation (1) to calculate the spin-polarized conductances across a multilayer in the P configuration as a function of the minority-spin potential $V_\downarrow$ for fixed $V_\uparrow$. This corresponds to considering magnetic materials with different exchange splittings. Results can be seen in figure 5(a). The parameters are the same as those used to obtain the $\uparrow$-spin transmission coefficient in figure 3, except for $V_\downarrow$, which varies from $V_\uparrow = 0.12$ up to $E_F = 0.23$. For $V_\downarrow = V_\uparrow = 0.12$ there is no contrast and both conductances are $\Gamma_P^\uparrow = \Gamma_P^\downarrow = 0.023$ (in units of e^2/h). However, as $V_\downarrow$ is increased towards E_F the concentration of minority-spin electrons in the magnetic material is reduced and its corresponding Fermi surface is shrunk. The conductance $\Gamma_P^\downarrow$, represented by a solid line in figure 5(a), reduces continuously and vanishes before $V_\downarrow$ reaches the Fermi level. The reduction of $\Gamma_P^\downarrow$ reflects the decreasing number of common conducting channels across the structure and $\Gamma_P^\downarrow$ goes to zero as soon as the minority-spin Fermi surface of the magnetic material fits into the centred opening of the spacer Fermi surface, shown in figure 4(b). When this happens the system acts as a spin filter, where $\downarrow$-spin electrons are blocked but $\uparrow$-spin ones are transmitted.

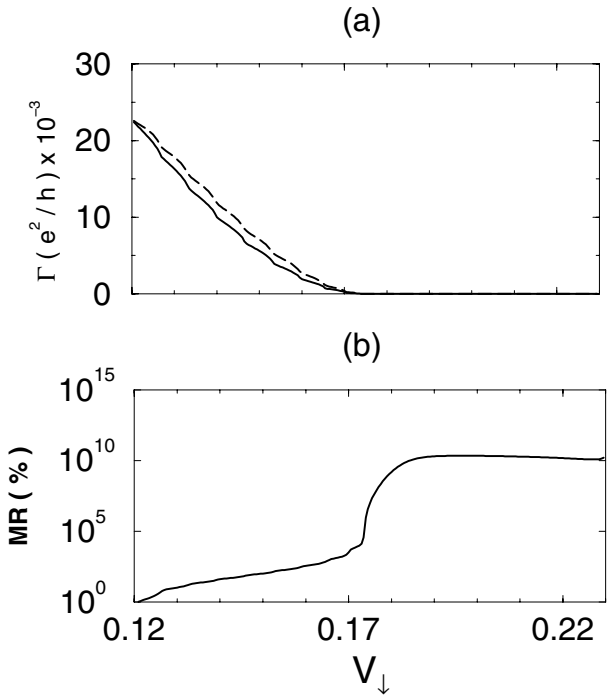

Figure 5. (a) Conductances $\Gamma_P^\downarrow$ (solid line) and $\Gamma_{AP}^{\uparrow\downarrow}$ (dashed line) as functions of the minority-spin potential $V_\downarrow$; (b) magnetoresistance as a function of $V_\downarrow$.

As pointed out before, a significant contrast between the spin-polarized conductances in the P configuration enhances the MR ratio. This becomes clear if we look at the expression for the MR ratio in terms of the spin-polarized conductances, which is given by

$$\mathrm{MR} = (\Gamma_P^\uparrow + \Gamma_P^\downarrow - 2\Gamma_{AP}^{\uparrow\downarrow})/(2\Gamma_{AP}^{\uparrow\downarrow}).$$

Since the magnetizations of the magnetic layers are reversed in the AP configuration, the

potential felt by ↑-spin electrons in one magnetic layer is equivalent to that seen by ↓-spin ones in the other. If a given spin-polarized current is blocked in the P configuration, it will also be blocked in the AP configuration. It is clear that when spin filtering occurs, $\Gamma_{AP}^{\uparrow\downarrow}$ should resemble $\Gamma_P^{\downarrow}$. The dashed line in figure 5(a) represents the conductance in the AP configuration for either spin polarization. In fact, both $\Gamma_P^{\downarrow}$ and $\Gamma_{AP}^{\uparrow\downarrow}$ go to zero simultaneously as the projected minority-spin Fermi surface fits into the opening of its spacer counterpart. Since we have kept $V_\uparrow$ fixed and varied just $V_\downarrow$, $\Gamma_P^{\uparrow}$ remains unaltered and the enhanced regime is reached when both $\Gamma_P^{\downarrow}$ and $\Gamma_{AP}^{\uparrow\downarrow}$ vanish. Strictly speaking, they are not exactly zero because of quantum tunnelling effects, but they can be very small leading to enormously large values of MR, as shown in figure 5(b). We point out that in the region where the conductances $\Gamma_P^{\downarrow}$ and $\Gamma_{AP}^{\uparrow\downarrow}$ are finite we have ordinary GMR.

Notice that the EGMR regime results from an ingenious combination of the spin-polarized electronic currents. In the P configuration, a spin-filtering effect blocks ↓-spin electrons but not the ↑-spin current. In the AP configuration both spin-polarized electrons are blocked and the system becomes insulating as far as the conduction along the modulation direction is concerned. It is remarkable that, although each component of the structure has metallic character and conducting channels, as a whole, the components have no common channels and the system is not conducting along the direction perpendicular to the layers. Furthermore, electrons are free to move along the in-plane direction in either configuration. An applied magnetic field makes the alignment of the magnetizations change from AP to P, resulting in a transition from insulating to spin-filtering phases. Such a magnetic-field-driven insulator-to-conductor transition is inherent to the appearance of the EGMR regime. It is worth highlighting that the insulating behaviour of the system in the AP configuration makes the respective resistances large, avoiding the experimental drawback of having to probe excessively small resistances.

Alternatively, for a given magnetic material, one can reach the EGMR regime by tuning the spacer modulation so that there are no bands in the transmission coefficient curve below E_F. This is equivalent to enlarging the centred opening of the projected spacer Fermi surface to embrace the projected minority-spin Fermi surface, suppressing all common conducting channels between them. To illustrate this situation we initially consider the same set of parameters as those used for obtaining the curves of figure 5. If, in addition, we assume that $V_\downarrow = 0.16$, according to figure 5, we fall into the GMR regime, where $\Gamma_P^{\uparrow}$ and $\Gamma_P^{\downarrow}$ are finite. By changing the modulation period to $a = b = 4.22$ the position of the gap is lowered in energy and both spin-polarized transmission curves in the P configuration are shown in figure 6. Because $V_\uparrow$ and $V_\downarrow$ differ by the exchange splitting of the spin-polarized sub-bands, they impose different cut-offs above which the system can conduct. For this reason, the lowest transmission band in $T_P^{\downarrow}$ is suppressed but not that in $T_P^{\uparrow}$, as shown in figure 6. As discussed previously, the conductance vanishes if there are no transmission bands below E_F. Spin filtering thus occurs for $E_F = 0.23$ since $\Gamma_P^{\downarrow}$ vanishes but not $\Gamma_P^{\uparrow}$. For $a = b = 4.22$ the opening of the corresponding Fermi surface is larger, having no common channel with the minority-spin Fermi surface of the magnetic material. Results for different values of a and b ($a = b$) show that the MR reaches the enhanced regime somewhere in between $a = b = 4.0$ and $a = b = 4.22$. More precisely, it arises at a certain value of a and b for which the bottom of the transmission gap coincides with the cut-off given by $V_\downarrow$. This is displayed in figure 7, where the MR ratio is plotted as a function of the length a ($a = b$). The EGMR regime is triggered for $a \approx 4.19$ reaching values as large as $10^7\%$. Clearly, the ordinary GMR regime is restored if we vary a and b further, because the transmission gap keeps moving to the left up to the point where the spin filtering in the spin-polarized conductances disappears.

As far as the contrast between the spin-polarized conductances is concerned, perfect spin

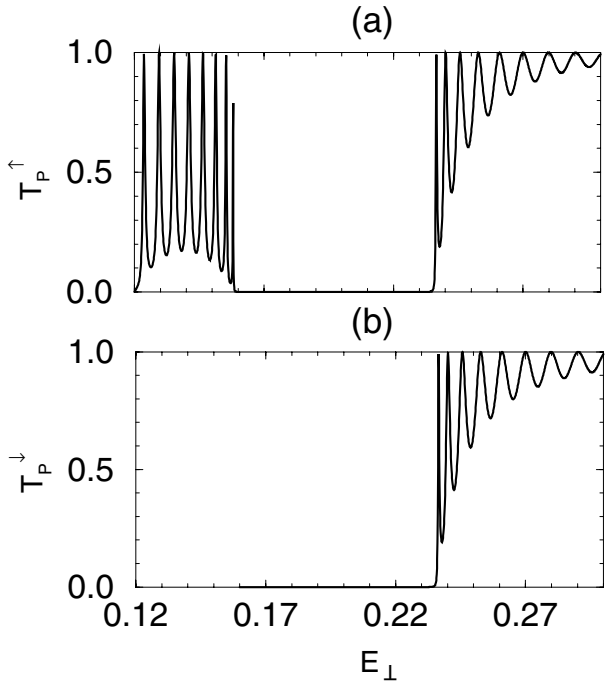

Figure 6. Transmission coefficients as functions of $E_\perp$ for $a = b = 4.2$. (a) $T_P^{\uparrow}$; (b) $T_P^{\downarrow}$.

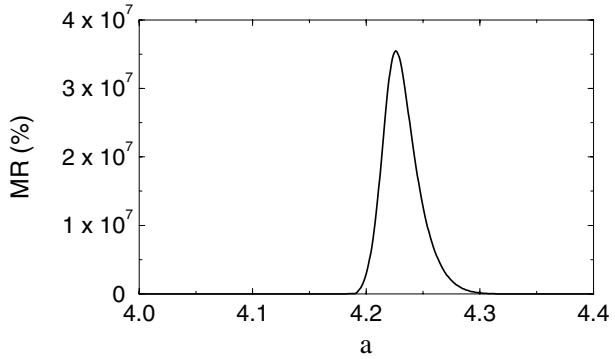

Figure 7. Magnetoresistance as a function of the thickness a (see the text).

filtering is the ideal situation, where only one spin-polarized current is allowed to travel across the system. Strictly speaking however, the other spin-polarized current is not entirely blocked but it is finite due to tunnelling effects. Thus, within the EGMR regime one can enhance the MR ratio by reducing the tunnelling of the non-conducting current. This can be achieved by thickening the modulated spacer. Figure 8(a) shows the conductances $\Gamma_P = \Gamma_P^{\uparrow} + \Gamma_P^{\downarrow}$ (filled circles) and $\Gamma_{AP} = \Gamma_{AP}^{\uparrow} + \Gamma_{AP}^{\downarrow}$ (empty circles) as functions of the number of cells in the spacer. Notice that Γ_P remains of the same order of magnitude whereas tunnelling states across the structure lead to exponentially decreasing Γ_{AP}. Such a difference gives rise to exponentially growing MR ratios, which can be seen from a plot of the MR as a function of the number of cells in the spacer (figure 8(b)).

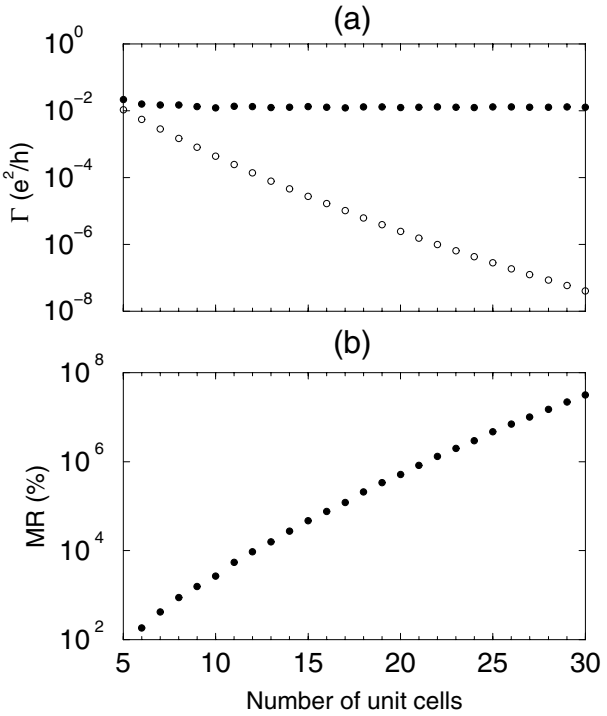

Figure 8. (a) Conductances $\Gamma_P = \Gamma_P^{\uparrow} + \Gamma_P^{\downarrow}$ (filled circles) and $\Gamma_{AP} = \Gamma_{AP}^{\uparrow} + \Gamma_{AP}^{\downarrow}$ (empty circles) as functions of the number of cells in the spacer. (b) Magnetoresistance as a function of the number of cells in the spacer.

4. Saturating magnetic fields

A question that naturally arises is that of what the saturating magnetic field is. This field is related to the interlayer exchange coupling between the magnetic layers, which has been intensively discussed in the literature [4]. The magnetic coupling between the layer magnetizations across the non-magnetic material separating them oscillates between parallel and antiparallel as the thickness of the spacer layer is changed. In addition, the amplitude of the oscillations slowly decays as the magnetic layers become far apart. The oscillation periods as well as the decay rate of the coupling are dependent on the shape of the Fermi surface of the non-magnetic material. They depend on certain properties of a few portions of the Fermi surface, namely, on its stationary wave vectors along the growth direction. More specifically, critical spanning wave vectors perpendicular to the layers linking two points of the bulk spacer Fermi surface with antiparallel velocities are the only ones which effectively contribute to the coupling [16].

Practical magnetic sensors require relatively low switching fields, which may be accomplished by engineering spin-valve sandwich structures made with soft magnetic layers weakly coupled to each other through a non-magnetic spacer [17]. This requires the spacer layer to be sufficiently thick. However, since the occurrence of the EGMR results from conduction in the ballistic regime, it is important to keep the non-magnetic spacer layer thinner than the average spin-dependent electronic mean free paths. When both conditions are met, the EGMR can be achieved with low fields. For such purposes, a rapidly decaying interlayer coupling may

be useful. It is noteworthy that when the Fermi surface of the superlatticed spacer develops openings along the modulation direction those critical wave vectors may not exist. In such a case, the spacer Fermi surface does not meet the criteria for contributing to the coupling with a slowly decaying oscillatory term, and the amplitude of the coupling decays exponentially with the spacer thickness [18]. This allows very weak coupling across relatively thin modulated spacers, which may be important for having the ballistic regime required by the EGMR to be effective. As pointed out before, small switching magnetic fields and large MR ratios form a highly attractive combination from the technological viewpoint.

5. Conclusions

A new regime of CPP magnetoresistance in systems made of magnetic layers separated by non-magnetic modulated spacers has been studied. The origin of this new regime lies in the role played by the energy gaps of the electronic structure of the modulated spacer. We have shown that by making an adequate choice of modulation periods and potential strengths one can produce contrasting spin-dependent conductances. When the system acts as a spin filter, the contrast is maximum and the magnetoresistance reaches extremely large ratios. The enhancement of the magnetoresistance ratios involves ingenious combinations of spin-polarized currents and is associated with a magnetic-field-induced metal–insulator transition along the modulation direction, characterizing a highly anisotropic transport behaviour. The existence of an insulating phase in this new regime circumvents the experimental challenge of probing excessively small resistances in the CPP magnetoresistance.

We have shown that the effect can be understood on the basis of a picture in terms of the bulk Fermi surfaces of the magnetic material and of the modulated spacer. Within the ballistic regime of electronic transport, each transverse mode that is conducting across the system works independently, acting as a collection of channels in parallel. The spin-filtering effect, essential for the occurrence of the EGMR regime, arises when the minority-spin Fermi surface of the magnetic material fits into the opening of that of the modulated spacer. In that case, minority-spin electrons cannot travel across the spacer and the system behaves as an insulator for those spin-polarized electrons. Having common channels with the spacer, the majority-spin electrons, on the other hand, are not blocked and the structure is conducting for those carriers. The picture in terms of the Fermi surfaces provides general guidelines on how to produce the spin-filtering effect and, consequently, on how to trigger the enhanced regime. The simple model that we have used to describe the electronic structure explains the origin of the EGMR regime and its relation to the modulation character of the system only qualitatively. More realistic calculations will be important for providing information concerning the proper matching of spin-polarized conducting channels between the ferromagnets and modulated structure, necessary to achieve the EGMR regime in specific systems. We hope that our work will stimulate experiments and further theoretical investigations in this field.

Acknowledgments

We wish to thank A Bruno Alfonso for helpful discussions. Financial support from CNPq and FAPERJ (Brazil), the Brazilian Academy of Science and the Royal Society (UK) is gratefully acknowledged.

Appendix

In the free-electron model, the expression for the transmission coefficient of a one-dimensional potential of the type shown in figure 2 can be easily calculated analytically. It can be cast in a very simple form by expanding the wave functions in terms of $\sin(kz)$ and $\cos(kz)$ rather than the usual canonical basis $\exp(\pm ikz)$ [19]. The matrix representing the propagation through a barrier A is then real and given by

$$A = \begin{pmatrix} \cos(k_A a) & -\sin(k_A a)/k_A \\ k_A \sin(k_A a) & \cos(k_A a) \end{pmatrix} \tag{A.1}$$

where

$$k_A = \sqrt{2m(E_\perp - V_A)/\hbar^2}.$$

A similar matrix, obtained by substituting

$$k_B = \sqrt{2m(E_\perp - V_B)/\hbar^2}$$

for k_A describes the propagation through each B barrier. The conductance through a superlatticed potential well containing n repeats of the superlattice unit cell is then given by

$$\Gamma = \frac{e^2}{h} \frac{4k/k'}{(M_{11} + M_{22})^2 + (M_{12} - M_{21})^2} \tag{A.2}$$

where M_{ij} $(i, j = 1, 2)$ is the element ij of the matrix

$$M = \begin{pmatrix} \cos(k_A a) & -\sin(k_A a)/k_A \\ k_A \sin(k_A a)/k & \cos(k_A a)/k \end{pmatrix} B(AB)^{n-1} \begin{pmatrix} \cos(k'L) & \sin(k'L) \\ -k' \sin(k'L) & k' \cos(k'L) \end{pmatrix} \tag{A.3}$$

where k and k' are the wave vectors for propagation through the magnetic layers and $L = n(a + b)$ is the total length of the superlatticed spacer.

References

[1] Prinz G A 1998 *Science* **282** 1660

[2] Baibich M N, Broto J M, Fert A, Nguyen van Dau F, Petroff F, Etienne P, Creuzet G, Friederich A and Chazelas J 1988 *Phys. Rev. Lett.* **61** 2472

[3] Berkowitz A E, Mitchell J R, Carey M J, Young A P, Zhang S, Spada F E, Parker F T, Hutten A and Thomas G 1992 *Phys. Rev. Lett.* **68** 3745
Xiao J Q, Jiang J S and Chien C L 1992 *Phys. Rev. Lett.* **68** 3749

[4] Grünberg P, Schreiber R, Pang Y, Brodsky M N and Sowers H 1986 *Phys. Rev. Lett.* **57** 2442
Parkin S S 1991 *Phys. Rev. Lett.* **67** 3598
Edwards D M, Mathon J, Muniz R B and Phan M S 1991 *Phys. Rev. Lett.* **67** 493
Edwards D M, Mathon J, Muniz R B and Phan M S 1991 *Phys. Rev. Lett.* **67** 1476 (erratum)
Edwards D M, Mathon J, Muniz R B and Phan M S 1991 *J. Phys.: Condens. Matter* **3** 3941

[5] Schep K M, Kelly P J and Bauer G E W 1998 *Phys. Rev.* B **57** 8907

[6] Prinz G A 1995 *Phys. Today* **48** (4) 58

[7] Himpsel F J, Ortega J E, Mankey G J and Willis R F 1998 *Adv. Phys.* **47** 511

[8] Schad R, Potter C D, Belien P, Verbanck G, Moshchalkov V V and Bruynseraede Y 1994 *Appl. Phys. Lett.* **64** 3500

[9] Mathon J 1996 *Phys. Rev.* B **54** 55
Mathon J 1997 *Phys. Rev.* B **55** 960

[10] Jin S, Tiefel T H, McCormack M, Fastnacht R A, Ramesh R and Chen L H 1994 *Science* **264** 413

[11] Fontcuberta J 1999 *Phys. World* **12** (2) 33

[12] Ferreira M S, d'Albuquerque e Castro J, Muniz R B and Villeret M 1999 *Appl. Phys. Lett.* **75** 2307

[13] Guo Y, Li Z-Q, Gu B-L, Sun Q, Yu J-Z and Kawazoe Y 1998 *Eur. Phys. J.* B **3** 263

[14] Guo Y, Gu B-L, Li Z-Q, Sun Q and Kawazoe Y 1998 *Eur. Phys. J.* B **3** 257

[15] El Boudouti E H, Djafari-Rouhani B, Akjouj A, Dobrzynski L, Kucharczyk R and Steślicka M 1997 *Phys. Rev.* B **56** 9603
[16] Bruno P and Chappert C 1991 *Phys. Rev. Lett.* **67** 1602
Bruno P and Chappert C 1992 *Phys. Rev.* B **46** 261
[17] Dieny B 1994 *J. Magn. Magn. Mater.* **136** 335
[18] Ferreira M S, d'Albuquerque e Castro J, Muniz R B and Lopes L C 1998 *Phys. Rev.* B **58** 8198
[19] de Oliveira P M C, Albuquerque E L and Mariz A M 1996 *Physica* A **227** 206